FILAMENT STRETCHING OF PRESSURE SENSITIVE ADHESIVES WITH GAS INCLUSIONS: A 3D HYPERELASTIC-VISCOELASTIC MODEL AND NUMERICAL SIMULATIONS

Yannis Dimakopoulos[*], John Papaioannou[*] & John Tsamopoulos[*a)]
[*]*Laboratory of Computational Fluid Dynamics, Department of Chemical Engineering, University of Patras, Patras, 26504, Greece*

Summary Debonding mechanisms during stretching of pressure sensitive adhesives start with cavitation and growth of cavities, continue with fibril formation and extension, and terminate with fibril breakage. How the competing viscoelastic and elastic forces determine the shape and tack properties of a stretched adhesive is predicted from the solution of the transient equations of mass and momentum conservation along with a nonlinear integral constitutive law (e.g. the mixed neo-Hookean/Maxwell model). These are solved numerically via 3D Lagrangian finite elements which account for the entire deformation history of the material. The geometry that we study, assumes the presence of a cluster of cavities with fixed contact lines with the bottom substrate. These are initially growing spherically, later like mushrooms and finally they are elongated axially forming fibrils or a foamy network. The radial growth of these cavities is significantly larger compared with that of cavities which are initially located in the mid-plane.

INTRODUCTION

Thin films of materials made by block copolymers (such as those based on acrylates) are widely used nowadays in a variety of applications as self-adhesives or pressure sensitive adhesives (PSAs). PSAs, in particular, have the ability to average stresses over large volumes of material, thus avoiding the sharp stress concentrations responsible for the failure of structural glassy adhesives. Controlling their stickiness or tackiness is important, since it governs their suitability in non-structural bonding applications. In PSAs, for example, a high degree of tackiness is required; in contrast, in coatings and paints, which are roughly made by similar polymers, a lower degree of stickiness is desired. Stickiness or tackiness is quantified in terms of the energy dissipated during the bonding-debonding cycle or in terms of the force required to separate a probe from the polymer film. Experimental measurements [1,2] show that the tack energy in many cases can be very high and this has been associated with a strong viscoelastic dissipation in the polymer film. This dissipation is either due to a fracture that propagates along the interface with the substrate or due to the polymer film being split into separate fibrils during the debonding process. In the latter case, when fibrillation occurs during debonding, measured stress vs. strain curves exhibit a strong peak and then a fall which does not go to zero; it rather approaches a low asymptote or even rises slightly till the probe finally separates from the film at a relatively high deformation [3,4].

PHYSICAL MODELING

Debonding mechanisms during stretching of pressure sensitive adhesives (PSAs) start with cavitation and growth of cavities, continue with fibril formation and extension, and terminate with fibril breakage. How the competing viscoelastic and elastic forces determine the growth of bubbles, the shape and tack properties of a stretched adhesive is predicted from the solution of the transient equations of mass and momentum conservation for an incompressible material,

$$det\left(\underline{\underline{F_o}}(t)\right) = 1 \tag{1}$$

$$\rho \frac{\partial^2 \underline{x}}{\partial t^2} = -\nabla \cdot \underline{\underline{\sigma}} \tag{2}$$

where ρ is the density of the PSA sample, $\underline{x}$ is the position vector at time t, $\underline{\underline{\sigma}}$ is the total stress tensor, ∇ is the gradient tensor, $\underline{\underline{F_o}}(t) = \partial \underline{x}(t)/\partial \underline{x}(t_o)$ is the relative deformation tensor. The deformation of the sample in response to an applied force during a stretching experiment depends on the non-linear elastic properties of the macromolecular network. According to Jensen et al. [5], the accurate description of these properties requires the combination of a hyperelastic and a viscoelastic Maxwellian model described as:

$$\underline{\underline{\sigma}} = -p\underline{\underline{I}} + \underline{\underline{\tau}}_{he} + \underline{\underline{\tau}}_{ve} \tag{3}$$

The hyperelastic stress is given by the general formula

$$\underline{\underline{\tau}}_{he} = \frac{\partial W}{\partial \underline{\underline{F_o}}} \underline{\underline{F_o}}^{\mathrm{T}}(\mathrm{t}) \tag{4}$$

where W is the strain energy function per unit undeformed volume for isotropic hyperelastic incompressible materials in terms of the first, I_1 of the Finger tensor $\underline{\underline{B_o}}(t) = \underline{\underline{F_o}}(t)\underline{\underline{F_o}}^T(t)$. Several models have been proposed for the strain energy function, e.g. the Neo-Hookean model $W = G(I_1 - 3)$. All exhibit a monotonic strain-hardening behavior.
The viscoelastic contribution follows the integral Maxwell constitutive equation

$$\underline{\underline{\tau}}_{ve} = \int_{-\infty}^{t} M(t-t')(\underline{\underline{I}} - \underline{\underline{B}}_{t'}(t))dt' \tag{5}$$

a) Corresponding author. Email: tsamo@chemeng.upatras.gr

where $M(t-t')$ is the memory function, $\underline{\underline{B}}_{t'}(t)$ is the Finger tensor.

LAGRANGIAN FINITE ELEMENT METHOD

The numerical method that we have adopted for the solution of the equations (1)-(5) is the Lagrangian finite element method [6]. In particular, the nodes of the mesh are moving with a velocity equal to the local velocity of the sample, while the governing are weighted according to the Galerkin principle. The discretization of the computational domain is based on tetrahedron elements after the tessellation of the control volume with an advancing-front algebraic mesh generator. Tetrahedron elements are preferred because they conform better to large deformations of the physical domain and can sustain larger distortions than the hexahedron ones without making the Jacobian of the local transformation to the parent element singular, especially around the contact curve of the cavity with substrate or around the bubbles. Moreover, the Taylor-Hood combination for the basis functions of the position vector and pressure is adopted for the satisfaction of the inf-sup LBB condition. Therefore, the weak form of the momentum balance for each finite element is given as follows:

$$\int_\Omega \rho\left[\frac{\partial^2 \underline{\underline{x}}}{\partial t^2} - \underline{g}\right]\phi^i d\Omega - \int_\Omega p\nabla\phi^i d\Omega - \int_\Omega \left(\underline{\underline{\tau}}_{he} + \underline{\underline{\tau}}_{ve}\right)\cdot(\nabla\phi^i)d\Omega + -\int_\Gamma [\underline{n}\cdot\underline{\underline{\sigma}}]\,\phi^i d\Omega = 0 \qquad (6)$$

where ϕ stands for the basis function of the position vector. The viscoelastic term $\underline{\underline{\tau}}_{ve}$ needs special treatment due to the time integral.

To approximate it accurately having the minimum possible computational cost, we adopt alternatively the Trapezoid or Simpson methods. The integral that ranges from $(-\infty, t]$ is divided into small intervals of varying size equal to the temporal time integration step dt

$$\int_\Omega \underline{\underline{\tau}}_{ve}\cdot(\nabla\phi^i)d\Omega = \int_\Omega \sum_{l=0}^{Nt}\int_{t_{l-1}}^{t_l} M(t-t')(\underline{\underline{I}} - \underline{\underline{B}}_{t'}(t))dt'\cdot(\nabla\phi^i)d\Omega \qquad (7)$$

dt is adjusted at each time-step based on the algorithms proposed by Dimakopoulos & Tsamopoulos [7].

The Jacobian matrix of each sub-problem that results after the application of the Newton-Rapshon solution technique along with a numerical calculation of all partial derivatives, is stored in Compressed Sparse Row (CSR) format and the linearized system is solved by using PARDISO, a robust direct sparse matrix solver.

RESULTS AND DISCUSSION

We assume that the PSA samples initially are cylindrical and contain fifteen cavities on the substrate. The top surface of the sample is pulled with a constant velocity, while the bottom surface adheres permanently on the substrate. Both top and bottom substrates are assumed to be non-slippery. The bubbles are initially growing spherically, later like mushrooms and finally they are elongated axially forming fibrils or a foamy network. The radial growth of these cavities is significantly larger compared with that of cavities which are initially located in the mid-plane. Therefore, their interplay is more important and affects both their shapes and the shape of the lateral surface. Apparently, due to the significant lowering of the pressure on the center line, the central cavities are growing faster than the surrounding ones. On the contrary, the expansion of the peripheral cavities is constricted both by the shrinking of the lateral sides of the adhesive and the fast expansion of the central cavity. Definitely, their final volume depends on their initial location and the distance between neighboring cavities.

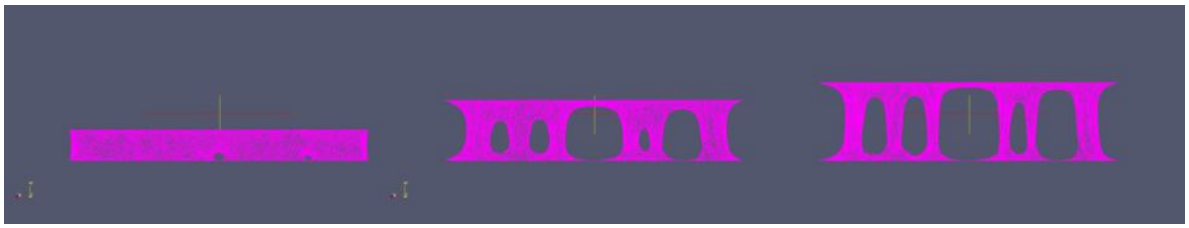

Figure 1: Snapshots of a filament stretching simulation of a PSA modelled as a neoHookean/Maxwell material, initially containing fifteen semispherical cavities on the bottom substrate of the sample. A vertical cross section is shown containing the axis of the sample.

References

[1] Dahlquist C.A., in: Patrick (Ed.), Treatise on adhesion and adhesives, Dekker, New York, 1969.

[2] Good, R.J., Gupta R.K.: *J. Adhes* **26**:13-36, 1988.

[3] Foteinopoulou K., Mavrantzas V.G., Dimakopoulos Y., Tsamopoulos J.: *Phys. Fluids* **18** (**4**): art. n. 042106 1-24, 2006.

[4] Lakrout H., Sergot P., Creton C.: *J. Adhesion* **69** (**3-4**):307-359, 1999.

[5] Jensen M.K, Rasmussen H.K., Skov A.L., Bach A., Kodbech H.: *Rheol. Acta* **49**:1–13, 2010.

[6] Rasmussen H.K.: *J. Non-New. Fluid Mech.* **84**:217-232, 1999.

[7] Dimakopoulos Y., Tsamopoulos J.: *J. Comp. Physics* **192**:494-522, 2003.

[a] Corresponding author. Email: tsamo@chemeng.upatras.gr